Silicon-photonics light source realized by III-V/Si grating-mirror laser

Chung, Il-Sug; Mørk, Jesper

Link back to DTU Orbit

Silicon-photonics light source realized by III–V/Si-grating-mirror laser

Il-Sug Chung[a)] and Jesper Mørk
*Department of Photonics Engineering, DTU Fotonik, Technical University of Denmark,
DK-2800 Kgs. Lyngby, Denmark*

A III–V/Si vertical-cavity in-plane-emitting laser structure is suggested and numerically investigated. This hybrid laser consists of a distributed Bragg reflector, a III–V active region, and a high-index-contrast grating (HCG) connected to an in-plane output waveguide. The HCG and the output waveguide are made in the Si layer of a silicon-on-insulator wafer by using Si-electronics-compatible processing. The HCG works as a highly-reflective mirror for vertical resonance and at the same time routes light to the in-plane output waveguide. Numerical simulations show superior performance compared to existing silicon light sources. © 2010 American Institute of Physics. [doi:10.1063/1.3503966]

A laser diode structure that can act as a light source for planar Si photonic circuits and can be monolithically integrated with Si-based electronics, will be a key building block in several important applications such as optical interconnects for computing, and lab-on-a-chip photonics for diagnosis of disease. For optical interconnect applications, the bandwidth is expected to reach the Tb/s range, requiring wavelength division multiplexing with, e.g., 25 lasers.[1] Thus, it is highly desirable for the laser source to feature single-wavelength emission,[1] low power consumption,[2] uncooled continuous-wave (CW) operation at typical processor temperatures of 70 °C–80 °C, and capability of high speed direct modulation. Thanks to the efficient light generation in III–V semiconductor direct band gap materials and the advent of hybrid wafer bonding technologies, a hybrid Si/III–V laser approach is likely to be the solution at least in the near future. Recently reported hybrid evanescent edge-emitting lasers incorporating distributed feedback and distributed Bragg reflector (DBR) structures demonstrated single-wavelength output power level of 5.4 mW and 11 mW, respectively.[1] However, their respective threshold currents, I_{th} of 25 mA and 65 mA and maximum CW lasing temperatures, T_{max} of 50 °C and 45 °C (Ref. 1) need to be further improved. Another hybrid laser employing a microdisk structure demonstrated prospects for optical logic gates.[3] However, its low differential efficiency and submilliwatt output power at room temperature is not sufficient for interconnect applications.

Here, we suggest a laser structure based on a vertical cavity resonance that emits light to an in-plane waveguide, hereafter called vertical-cavity in-plane-emitting laser (VCIEL). So far, a hybrid laser structure employing a vertical laser cavity has not been reported though the vertical cavity approach is advantageous for low power consumption and high-speed direct modulation. This may be attributed to the fact that the achievement of in-plane light emission from a vertical laser cavity is not straightforward. In the suggested structure, in-plane emission is realized by employing a recently-reported high-index-contrast grating (HCG) as a reflector as well as a router. The HCG is a one- or two-dimensional photonic crystal slab surrounded by a low re-

fractive index material.[4] As shown in Fig. 1(a), the suggested VCIEL structure consists of a DBR, a III–V active region, and a HCG that is connected to an in-plane output waveguide. Both the HCG and the in-plane waveguide are made in the Si layer of a silicon-on-insulator (SOI) substrate. This HCG reflects most of the vertically-incident light, e.g., 99.5%, as well as routing a small fraction of the vertically incident light, e.g., 0.17%, to the in-plane output waveguide. The mode profile of this laser structure, shown in Fig. 1(b), clearly shows that a strong vertical resonance occurs between the DBR and the HCG simultaneously with the routing of light laterally to the in-plane output waveguide. This output waveguide is placed into the right of the HCG, cf. Fig. 1(a), overlapping with the tail of the optical mode and ensuring routing only to the right.
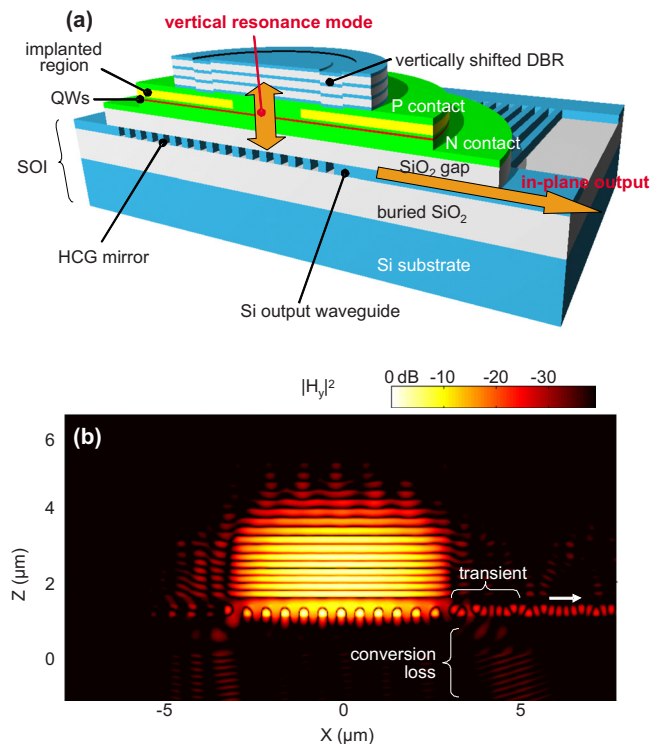

FIG. 1. (Color online) (a) Schematic profile of the VCIEL structure. (b) Normalized mode profile $|H_y|^2$ of the fundamental mode.
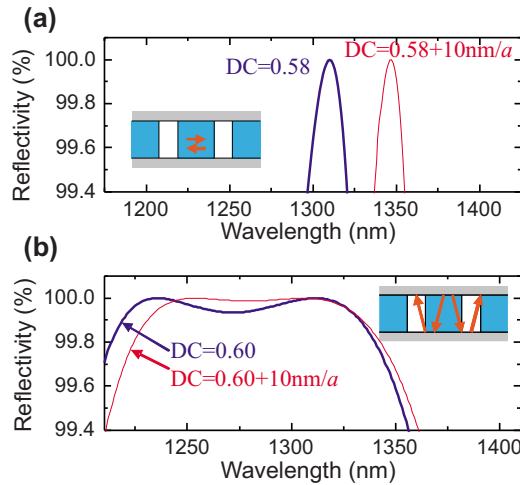
FIG. 2. (Color online) Reflectivity spectra (blue thick) of (a) a slow HCG with a=730.5 nm, h=250 nm, and DC=0.58 and (b) the fast HCG employed in this paper, without the in-plane waveguide connected. The red thin curves show the result of increasing the DC by 10 nm/a.

FIG. 3. (Color online) Normalized Poynting vector profiles for a fast HCG (a) near the central part and (b) near the in-plane output waveguide.

Let us describe further the laser structure. The 3λ-long active region including five 6.6-nm-thick InAlGaAs quantum wells (QWs) optimized for high temperature operation, is almost identical to that of 1.31-μm-wavelength vertical-cavity surface-emitting lasers (VCSELs).[5,6] This active region with a 186-nm-thick SiO$_2$ gap layer deposited, is wafer-bonded[7] to the prepatterned SOI wafer. No bonding alignment is required. The DBR (five-pair Si/SiN and a SiC layer) is deposited to the active region. The optical confinement is obtained by the vertically shifted DBR rim which has inner and outer diameters of 6 and 10 μm and is prepared by etching a 102-nm-deep dip before the DBR deposition. The 5-μm-diameter current aperture is formed by proton implantation. A 2-μm-thick Cu heat spreader with a 0.5 μm Au seed layer[8] is formed, as shown in Fig. 4(b). The buried SiO$_2$ layer is 1-μm-thick. The employed HCG has period, a =515 nm, thickness, h=355 nm, and a duty cycle (DC) =0.6, corresponding to the filling ratio of Si. All processing steps are compatible with VCSEL fabrication technologies.

For optical simulations, a two-dimensional finite-difference time-domain method is used to obtain the lasing wavelength, threshold gain, mode profile, and various losses. Our method reproduces experimental results for HCG and HCG VCSELs,[4,9] and was used to design various HCG VCSELs.[5,10] The spatial grid sizes for transverse and longitudinal directions are both 10 nm. For thermal simulations, a three-dimensional finite element method with rotational symmetry is used to obtain the temperature distribution and thermal resistance. This approach reproduces the measured thermal resistance, R_{th} of the aforementioned reference VCSEL device.[6] The experimental results of this reference VCSEL (Refs. 5 and 6) are used to calibrate the power-current (L-I) curve of the VCIEL.

The physical characteristics of the HCG are key to the VCIEL performance, and we classify highly reflective HCGs into slow and fast HCGs. In slow HCGs, the resonance of in-plane HCG modes, such as shown in the inset of Fig. 2(a), results in a high reflectivity,[11] while in fast HCGs, the resonance which involves vertically-propagating HCG modes, c.f. Fig. 2(b), does. The resonance of fast HCG modes has a shorter lifetime than that of slow HCG modes. It is because
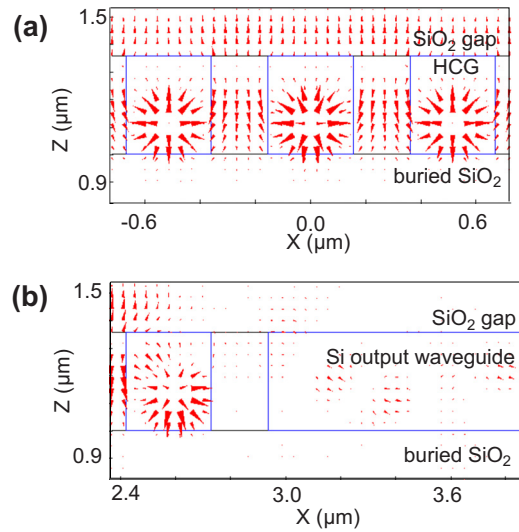
vertical propagation of fast HCG modes results in more transmission loss at HCG-air interfaces, per unit time, compared to the scattering loss to radiation modes, per unit time, experienced by laterally propagating slow HCG modes. The reflection delay time, τ_d measures the time taken for incident light to be reflected from a HCG,[5] and reflects this difference in resonance lifetimes. For example, a slow HCG with a =730.5 nm, h=250 nm, and DC=0.58 has τ_d^s=3.0t_r^s, while the fast HCG employed here has τ_d^f=1.3t_r^f, where $t_r^{s,f}$ denote vertical round-trip propagation times in the respective HCG slabs, assuming averaged uniform refractive indices. Figure 2 compares the reflectivity spectra of these exemplary slow and fast HCGs and their sensitivity to the DC variation. As a result of the shorter resonance lifetime and a double resonances at λ=1236 and 1312 nm, the fast HCG has a broader $\Delta\lambda_{R\geq 99.9\%}$=140 nm than the slow HCG. Due to the larger $\Delta\lambda$ and the weaker resonance, the reflectivity spectrum of the fast HCG is less sensitive to the DC variation. A detailed experimental study of the fabrication tolerance of fast HCGs can be found elsewhere.[12] As shown in Fig. 3(a), the field flux in the middle of the fast HCG is spatially a standing-wave; the upward and downward modes, as well as toward-the-right and toward-the-left modes balance each other. However, there is only toward-the-right component in the end of the HCG shown in Fig. 3(b), which results in the routing of light to the in-plane output waveguide. This routing process is the same for the slow HCG. Since the slow HCG modes dwell in the HCG for a longer time, the slow HCG gives a coupling efficiency that is higher by approximately a factor of $\tau_d^s/\tau_d^f \approx 1.7$. In the suggested laser structure, we decide to employ the fast HCG despite of its smaller routing efficiency, since its broad $\Delta\lambda$ and smaller sensitivity to the DC variation, are desirable, due to thermal redshifting in the gain spectrum and relaxed fabrication tolerance, respectively.

The out-coupling efficiency, $F\eta_0$ (Ref. 13) is defined as the ratio of the in-plane output power and the sum of all losses including mirror, scattering, and absorption losses, and equals 18.5% for the specific design used here. The mode conversion from the HCG mode to the waveguide mode occurs in the *transient* region, shown in Fig. 1(b), and accom-
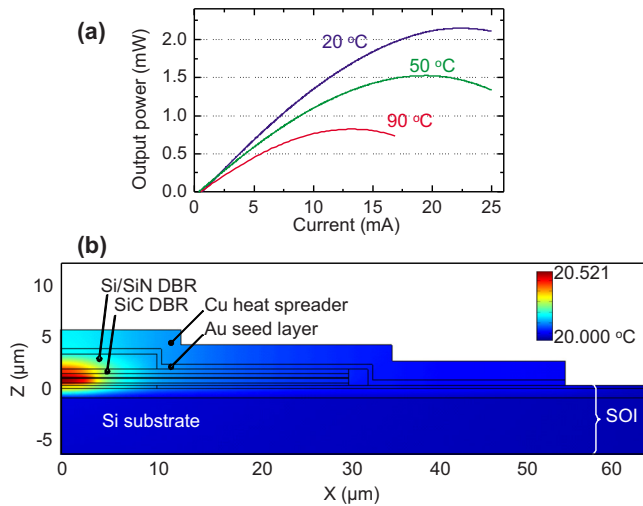
FIG. 4. (Color online) (a) *L-I* curves at different temperatures. (b) Temperature distribution at threshold.

panies the scattering underneath the HCG, due to mode mismatching. The amount of this conversion loss is 23.3% of the total loss and is expected to be considerably reduced by optimizing the topology of the transient region.[14] With a 3 dB reduction in the conversion loss, the efficiency will exceed 30%.

Power-current graphs at different temperatures are presented in Fig. 4(a). The submilliampere threshold currents result from the small active region volume and the high QW confinement factor of the VCIEL cavity compared to normal VCSEL structures. The high temperature operation is attributed to the high-temperature QW design and the low R_{th}. About 1 mW single-mode output at $70\ ^{\circ}C - 80\ ^{\circ}C$ is predicted with an electrical power input of about 18 mW (=10 mA×1.8 V). If this hybrid HCG VCIEL is directly modulated at 25 Gbps, the power consumption (light generation+modulation) per bit will be 0.8 pJ/bit.

The temperature distribution at threshold is presented in Fig. 4(b). It is assumed that the heat sink temperature, T_{snk}, i.e., the substrate bottom temperature is maintained at 20 °C, and that a heat of 0.66 mW (=$I_{th} \times V_{th}$) is generated near the current aperture, which is the case for the intracavity contacted structures. The Si/SiN DBR is modeled as a bulk material with an anisotropic thermal conductivity of (κ_r, κ_z) = (59, 29.5) W/K m. In Fig. 4(b), the high temperature contour extends farther toward the top DBR and the Cu/Au heat spreader than toward the SOI, which means that more heat is dissipated through the upper channel with high thermal con-

ductivity. The R_{th} is estimated by using the relation,[13] R_{th} =$(T_{src} - T_{snk})/P_{el}$, where T_{src} is the heat source temperature, i.e., the hottest temperature in the VCIEL. Its value is 0.79 °C/mW, which is even lower than state-of-the-art high temperature VCSELs with the same current aperture diameter[8] and is highly beneficial for high speed operation and long life time.[8]

In conclusion, we have suggested a hybrid laser structure for silicon photonics that exploits the properties of HCGs. The laser is based on hybrid wafer bonding but does not require alignment. Numerical simulations have shown that the suggested laser structure have submilliampere threshold current and about 1 mW single-mode output power at typical processor temperatures, and operates up to 110 °C. The output power at high temperature can be further improved by optimizing the topology of the HCG to the output waveguide and adjusting the gain offset with respect to the cavity wavelength. This structure is scalable to the 1.55 μm wavelength region.

[1]A. W. Fang, M. N. Sysak, B. R. Koch, R. Jones, E. Lively, Y.-H. Kuo, D. Liang, O. Raday, and J. E. Bowers, IEEE J. Sel. Top. Quantum Electron. **15**, 535 (2009).
[2]D. Miller, Proc. IEEE **97**, 1166 (2009).
[3]L. Liu, R. Kumar, K. Huybrechts, T. Spuesens, G. Roelkens, E.-J. Geluk, T. Vries, P. Regreny, D. V. Thourhout, R. Baets, and G. Morthier, Nat. Photonics **4**, 182 (2010).
[4]C. F. R. Mateus, M. C. Y. Huang, L. Chen, C. J. Chang-Hasnain, and Y. Suzuki, IEEE Photonics Technol. Lett. **16**, 1676 (2004).
[5]I.-S. Chung, V. Iakovlev, A. Sirbu, A. Mereuta, A. Caliman, E. Kapon, and J. Mørk, IEEE J. Quantum Electron. **46**, 1245 (2010).
[6]A. Sirbu, A. Mereuta, V. Iakovlev, A. Caliman, P. Royo, and E. Kapon, Proceedings of the Optical Fiber Communication Conference, 2008, San Diego, CA.
[7]Q.-Y. Tong, G. Fountain, and P. Enquist, Appl. Phys. Lett. **89**, 042110 (2006).
[8]A. N. AL-Omari, G. P. Carey, S. Hallstein, J. P. Watson, G. Dang, and K. L. Lear, IEEE Photonics Technol. Lett. **18**, 1225 (2006).
[9]M. C. Y. Huang, Y. Zhou, and C. J. Chang-Hasnain, Nat. Photonics **1**, 119 (2007).
[10]I.-S. Chung, J. Mørk, P. Gilet, and A. Chelnokov, IEEE Photonics Technol. Lett. **20**, 105 (2008).
[11]X. Letartre, J. Mouette, J. L. Leclercq, P. Rojo Romeo, C. Seassal, and P. Viktorovitch, J. Lightwave Technol. **21**, 1691 (2003).
[12]Y. Zhou, M. C. Y. Huang, and C. J. Chang-Hasnain, IEEE Photonics Technol. Lett. **20**, 434 (2008).
[13]L. A. Coldren and S. W. Corzine, *Diode Lasers and Photonic Integrated Circuits* (Wiley, New York, 1995).
[14]L. Yang, A. V. Lavrinenko, L. H. Frandsen, P. I. Borel, A. Têtu, and J. Fage-Pedersen, Electron. Lett. **43**, 923 (2007).